

JUN 18 1982

MASTER

POSITRON SCANNER FOR LOCATING BRAIN TUMORS\*

BNL 6041

S. Rankowitz, J. S. Robertson, W. A. Higinbotham and  
M. J. Rosenblum  
Brookhaven National Laboratory  
Upton, N.Y.

Summary

A system will be described which makes use of positron emitting isotopes for locating brain tumors based on the method developed by Sweet, Brownell and Aranow.<sup>1,2,3</sup> This system inherently provides more information about the distribution of radioactivity in the head in less time than existing scanners which use one or two detectors. A stationary circular array of 32 scintillation detectors scans a horizontal layer of the head from many directions simultaneously. The data, consisting of the number of counts in all possible coincidence pairs, is coded and stored in the memory of a Two-Dimensional Pulse-Height Analyzer.<sup>4</sup> A unique method of displaying and interpreting the data will be described which enables rapid approximate analysis of complex source distribution patterns.

Introduction

For a number of compounds, the rate of uptake by brain tissue is slower than the rate of uptake by muscle tissue or by certain types of tumor tissue. Thus, after intravenous injection of labeled compounds, the radioactivity may be higher temporarily in brain tumors than in surrounding healthy brain tissue. This phenomenon has been used to locate tumors in the head. The technique is difficult because the tracer level in the blood stream and in muscle tissue is comparable to that in the tumors; the activity ratios are small and the effect is transitory. The scanning has heretofore been done with one or two detectors so that it has taken a long time to accumulate data even when relatively large amounts of tracer have been injected.

Sweet, Brownell and Aranow<sup>1,2,3</sup> have used positron emitters as the radioactive tracers. An emitted positron gives rise,

through an annihilation reaction, to two 0.51 Mev gamma rays which are emitted in opposite directions. When detectors are placed on opposing sides of the source, a coincidence indicates activity within the cylindrical space connecting the detectors. This has several advantages compared with the use of a single gamma collimated detector, e.g. improved resolution and insensitivity to background single gamma radiation without the necessity of large, heavy shielding and collimating structures. The current work is an extension of this technique, making use of a multiplicity of detectors. This report covers four aspects of this development: 1) factors affecting arrangement of detectors, 2) electronic circuits for counting coincidences, 3) relating output data to activity distribution in the source, 4) preliminary results. The instrument is built and has been tested with artificially produced radiation patterns. It has yet to be tried on human patients, and the best method of analyzing and presenting the data has not been determined.

Arrangement of Detectors

Positron coincidence scanning with two detectors is illustrated in Fig. 1. The detector pair is scanned slowly up and down and forward and back registering the coincidence counts produced by positron annihilation gamma rays on a projection map of the head. A serious disadvantage of this kind of projection representation, also used with the single gamma scanning technique, is the distortion of the recorded radioactivity pattern which can result. In cases of

\* This work was done under the auspices of the U. S. Atomic Energy Commission.

## **DISCLAIMER**

**This report was prepared as an account of work sponsored by an agency of the United States Government. Neither the United States Government nor any agency Thereof, nor any of their employees, makes any warranty, express or implied, or assumes any legal liability or responsibility for the accuracy, completeness, or usefulness of any information, apparatus, product, or process disclosed, or represents that its use would not infringe privately owned rights. Reference herein to any specific commercial product, process, or service by trade name, trademark, manufacturer, or otherwise does not necessarily constitute or imply its endorsement, recommendation, or favoring by the United States Government or any agency thereof. The views and opinions of authors expressed herein do not necessarily state or reflect those of the United States Government or any agency thereof.**

## **DISCLAIMER**

**Portions of this document may be illegible in electronic image products. Images are produced from the best available original document.**

multiple tumors, the projections can be misleading even when two projections from different angles are taken.

Additional detectors are desirable to provide more information about the radioactivity pattern with greater speed, i.e. by simultaneously scanning from many directions. One possible configuration is shown in Fig. 2 with the detectors arranged in two planes on each side of the head. The number of coincidences equals  $\left(\frac{n}{2}\right)^2$ , where n is the

total number of detectors. This arrangement is more sensitive to counts at the center of the pattern than at the top and bottom, and some of the detectors are farther from the center than others. It was finally decided to arrange the detectors in a circle as shown in Fig. 3. The system has 32 detectors with 1 1/4 inch diameter by 1 inch deep NaI crystals arranged in a 15 inch diameter circle. Figure 3 shows the sensitive areas which intersect the head, for the coincidences between detector No. 1 and the opposing detectors. The head is, therefore, "scanned" simultaneously from each detector resulting in 9 to 11 paths through the head producing coincidences for each detector. An average head will produce about 170 to 180 coincidence combinations. This ring will take data in one plane and will be moved in 10 steps along the vertical axis of the head to obtain three-dimensional data.

#### Coincidence Pair Counting System

In addition to the detector counting assembly the system includes: 1) coincidence circuitry which counts coincident pulses between any pair of detectors and codes the data in a form suitable for storage in 2) a Two-Dimensional Pulse Height Analyzer memory.<sup>4</sup>

The detectors are numbered from 1 to 32 sequentially around the circumference. The coincidence counting system, using standard Computer Control Co. "S-Pacs"<sup>5</sup> and compatible laboratory-built circuitry,

examines each event, rejecting single counts and multiple coincident counts of three or greater, and finally codes the two detectors in the pair for memory storage. The lower number detector is coded in a train of pulses equal to its assigned number and stored in the X memory of the Two-Dimensional Analyzer. The higher number detector is simultaneously coded into another pulse train equal to its assigned number and stored in the Y memory.

Referring to the system block diagram (Fig. 4), each of the 32 detector amplifier outputs drives one input of a 2 input NAND circuit which in turn sets one stage of the 32 stage shift register. The other input is a gate common to all 32 input NANDS which can prevent setting of the shift register during analysis of an event.

When the input gate is open, any single or multiple coincident event<sup>(A)</sup> can set the appropriate shift register stages in parallel. The Clock Gate Flip-Flop<sup>(B)</sup> is set by the switching of any shift register stage through the 32 fold "OR" circuit. The input NAND gate closes immediately<sup>(R)</sup> preventing acceptance of any more detector pulses until completion of the analysis. The Clock Gate Flip-Flop triggers Pulse Shaper<sup>(C)</sup> which inhibits for 10µsec the start of the gate<sup>(F)</sup> to the Clock Multivibrator<sup>(G)</sup>. During this delay period, the states of all 32 stages of shift register are examined in parallel to determine whether the event was a single or a multiple coincidence. Since only the coincidence pair of 0.51 Mev annihilation gammas is of interest in this scan, the analysis of singles and all other multiple coincidences are prevented. The three standardized outputs from the coincidence analyzer, indicating the number of switched shift register stages, are converted in the logic NAND-NOR circuitry to a standard one or zero level voltage<sup>(D)</sup>; logic zero (0 volt) represents a coincidence pair, and logic one (-6 volts) represents a single or triple or

gher order coincidence. This voltage is gated in a 2 input NAND by a standard 0.6  $\mu$ sec pulse( $\bar{E}$ ) at the end of the 10  $\mu$ sec clock gate inhibit pulse. A coincidence pair will result in a closed gate. Any other condition opens the gate and permits the pulse( $\bar{E}$ ) to trigger a delay multivibrator which generates a 10  $\mu$ sec pulse( $L$ ) to reset the shift register, all flip-flops, and open the input gate.

The coding of the 2 detectors involved in a coincident pair proceeds by gating "ON" the free-running Clock Multivibrator after the 10  $\mu$ sec logic delay period. Shift pulses( $G$ ) are generated at about 600 kc. These shift pulses appear simultaneously at the X and Y outputs until the X Gate Scale-of-two is set( $K$ ). A 0.6  $\mu$ sec delay in triggering this scaler permits the last X pulse to appear at M. The number of shift pulses required to change the state of the No. 1 shift register equals the lower detector number involved in the coincidence pair. The No. 1 shift register stage( $H$ ) gates through a clock pulse( $I$ ) to trigger the X Gate Scale of 2. The shift pulses appear simultaneously at the X and Y outputs until the X Gate scaler is set, inhibiting the X output. The shift pulses continue until the No. 1 shift register stage again gates through a second clock pulse to trigger the X Gate Scaler, resetting it. Returning the scaler to its reset state resets the Clock Gate Flip-Flop and stops the clock. Therefore, the number of pulses in the Y train corresponds to the second detector number involved in the coincidence pair. Resetting the Clock Gate Flip-Flop triggers pulse shaping circuits; one( $L$ ) resets the shift register, and a second one generates a "STORE" pulse( $P$ ) to the Two-Dimensional Pulse-Height Analyzer Memory.

The "STORE" pulse transfers the X and Y register counts in the Pulse-Height Analyzer into the proper location of its magnetic drum memory. During this memory storage time, the Scanner input NAND's remain blocked( $R$ ). As a safety measure, to prevent

opening the input gates for the few microseconds between resetting the Clock Gate Flip-Flop and starting the "Dead Time" pulse, the 10  $\mu$ sec shift register reset pulse is applied to NOR( $R$ ). Upon completion of the "Dead Time" pulse the Scanner is able to accept a new input from the detectors.

#### Data Presentation and Analysis

The stored data in the Two-Dimensional Analyzer consisting of the number of coincident counts recorded in each pair of detectors, sorted into X (horizontal) and Y (vertical) coordinates, can be displayed on the analyzer oscilloscope as an intensity modulated two-dimensional map or as count magnitude curves of the X channels for any selected Y. The curves of any selected group of Y channels may be simultaneously displayed vertically displaced.

The most useful presentation for analyzing the data and locating the tumor is the X-Y map. The curves are used to determine amplitudes and channel groupings more accurately in doubtful regions, when necessary. The display map intensity modulation can be varied with the scale factor switch in binary steps to permit setting the threshold of visibility at different levels.

Although actual tumors behave as extended sources of radiation in an absorbing medium containing varying amounts of lower level radiation, the technique of locating tumors may be illustrated by first observing the coincidence data patterns produced by a point source. Refer to Fig. 5.

1. Point source in center: It is obvious that a point source in the center of the detector circle will produce an equal number of coincident counts in all opposite detector pairs. Since the opposite pairs are 16 detectors apart, the coincidence pattern will be a straight line of constant difference,  $Y-X = 16$ , plotted on Fig. 6 as curve 1.

2. Point source 1.5 inches from center on diameter 9-25: If all coincidences are plotted on X-Y coordinates, Curve 2 results. This curve intersects Curve 1, the line of constant differences at only one point, X = 9, Y = 25. Curve 3 results from the source at 3 inches from center on the same diameter. For both curves:

if  $X < 9$ ,  $(Y-X) < 16$   
and  $X > 9$ ,  $(Y-X) > 16$

The diameter on which the source is located is determined therefore by locating the counter pair for which  $Y-X = 16$ . The distance of the source from the center of the circle may be determined by observing the coordinates X, Y at which  $(Y-X)$  differs most from 16. The location of a point source in the scanned area is then determined by the intersection of the radial line for  $(Y-X) = 16$  and a line defined by any pair of coincidence detectors obtained from the coincidence curve. The coincidence curve as shown here appears on the display scope of the Two-Dimensional Analyzer.

The X, Y coincidence data provides a great deal of information about the location and size and shape of the tumor. A point source can clearly be accurately located. An extended tumor can be located by a similar analysis as long as the background level caused by radiation from surrounding brain tissue and blood is low enough to produce a contrast. A tumor of finite extent will produce a band on the display similar to that from a point source (Fig. 7) whose width is approximately proportional to the average diameter of the tumor. This band will intersect the reference curve  $Y-X = 16$  over some region of coordinates. The center of this intersection will determine the angle of the tumor from the center of the head, and the boundaries can be resolved by observing the outer coordinates along the band and plotting these coincidence lines between the detectors.

The following figures (8a to e) are Polaroid photographs of the Two-Dimensional Analyzer map display for some artificially produced patterns of radioactivity. Each figure contains three photographs of the same display, but with count scales of

27, 28, 29. The positron emitting isotope used as the source of tumor and background radiation is  $\text{Na}^{22}$ .

Figure (8a) shows the map display for three small (1/4 inch diameter) sources located on the diameter between detectors 9 and 25 at the center and at distances of 3 inches on either side of center with no background radiation. These correspond to curves plotted in Fig. 6.

The straight line,  $Y-X = 1$ , which appears on all photographs for the low count scale results from coincidences between adjacent detectors caused by the high energy single gammas emitted by  $\text{Na}^{22}$  and the proximity of the detectors. This well defined straight line, together with the zero axes, outlines the useful data area of the display. These coincidences are not useful analytically since they tell nothing about the source distribution.

It should be noted that data for  $Y = 32$  does not appear on these photographs because of the selection of display scales available.

Figure (8b) shows the map display for the same 1/4 inch diameter source in the center and a larger source (about 1 1/2 inches diameter) located 2 1/4 inches from center toward detector 9 on the same diameter as in Fig. (8a), with no background.

Figure (8c) shows the same conditions as Fig. (8b) but with a uniform background radiation throughout the head area.

Figure (8d) shows the same conditions as Fig. (8c), but with a third 1/4 inch diameter source (about 1/3 the intensity of the larger one), located on a diameter from 1 to 17 (front to back midline of head), at a distance of 3 inches from center toward detector 1. The curve for this source intersects the reference constant difference line at the XY coordinates 1, 17. Since it is less active than the larger source, it is not visible on the highest count scale.

Figure (8e) illustrates the kind of deductions that can be made about the shape as well as location of the tumor. Four Polaroid photographs of the coincidence data produced by an approximately elliptical tumor between the center and point 3 of Fig. 5 with scale ranges of  $2^7$  through  $2^{10}$  are shown in a uniform background. One edge of the band of X-Y data coincides with the straight line  $Y-X = 16$ , indicating on which side of center the source is located. The band crosses the reference line at  $(X, Y = 9, 25)$  indicating the major axis. Since the width of the band is definitely smallest in the region of  $(X, Y = 9, 25)$ , the source dimension perpendicular to this diameter is smaller than the dimension along the diameter. The width of the X-Y data band at the extremes indicates the approximate length of the source along the diameter (9, 25); the number of coincident pairs in the region of (9, 25) indicates the dimension perpendicular to this diameter.

Thus, by examining the characteristics of the coincidence data on the intensity modulated X-Y coordinate map, a great deal of information about the location, size and shape of the source of radioactivity can be readily obtained despite a high level of background.

A study program is being conducted to determine whether a mathematical solution of the problem of converting the coincidence data to a map of the radioactivity distribution with reasonable errors is feasible. One such method treats each of the N areas within the head (where N equals number of coincidence combinations caused by the radioactivity within the head) as though it were the component of an N dimensional vector. The mapping from the space of such vectors on to the space of coincidence counts is linear and consequently can be represented by a N x N matrix. If this matrix has a stable inverse it is then possible to convert the coincidence data unambiguously to a map of the radioactivity distribution using a simple computer program.

The inverse operation is degraded by statistical and system variations in the coincidence counts. It is too soon to tell whether this mathematical approach will prove to be practical. It is also possible that other modes of display may be advantageous.

#### References

1. G. L. Brownell and W. H. Sweet, "Localization of Brain Tumors with Positron Emitters," *Nucleonics*, Vol. 11, No. 11, pp. 40-45, (1953)
2. W. H. Sweet and G. L. Brownell, "Localization of Intracranial Lesions by Scanning with Positron-Emitting Arsenic," *J.A.M.A.* 157, 1183 (1955)
3. S. Aranow and G. L. Brownell, "An Apparatus for Brain Tumor Localization Using Positron-Emitting Isotopes," *IRE Convention Record*, Vol. 4, Part 9:8, (1956)
4. R. L. Chase, "A Two-Dimensional Kicksorter with Magnetic Drum Storage," *IRE Convention Record*, Part 9, p. 196, (1959)
5. Computer Control Co., Framingham, Mass.

### Figure Captions

1. Positron coincidence scanning with two detectors
  2. Positron coincidence scanning with detectors arranged in two planes on each side of the head
  3. Positron coincidence scanning with 32 detectors arranged in a circle
  4. Block diagram of coincidence detector pair coding system
  5. Positions of test sources for Figs. 6 and 7
  6. X-Y coincidence patterns derived from point sources at positions 1 through 5 on Fig. 5
  7. X-Y coincidence pattern for point source at center (1) and for 1.5 inch diameter source located between points 2 and 3 on Fig. 5
- 8a-e. Photographs of Two-Dimensional Analyzer map display. Count scales (top to bottom) are  $2^7$ ,  $2^8$ ,  $2^9$ . Point source used is 1/4 inch diameter
- (a) Three point sources located on diameter between detectors 9 and 25, at points 1, 3 and 5 of Fig. 5
  - (b) Point source at 1 and larger source between points 2 and 3 of Fig. 5
  - (c) Same as (b) but with uniform head background
  - (d) Same as (c) but with third source (point) located three inches toward front of head on front to back centerline
  - (e) Point source at 1, and approximately elliptical shaped uniform source in field of uniform head background; long axis of source is on 9, 25 diameter. Fourth photo taken with  $2^{10}$  counts full scale.



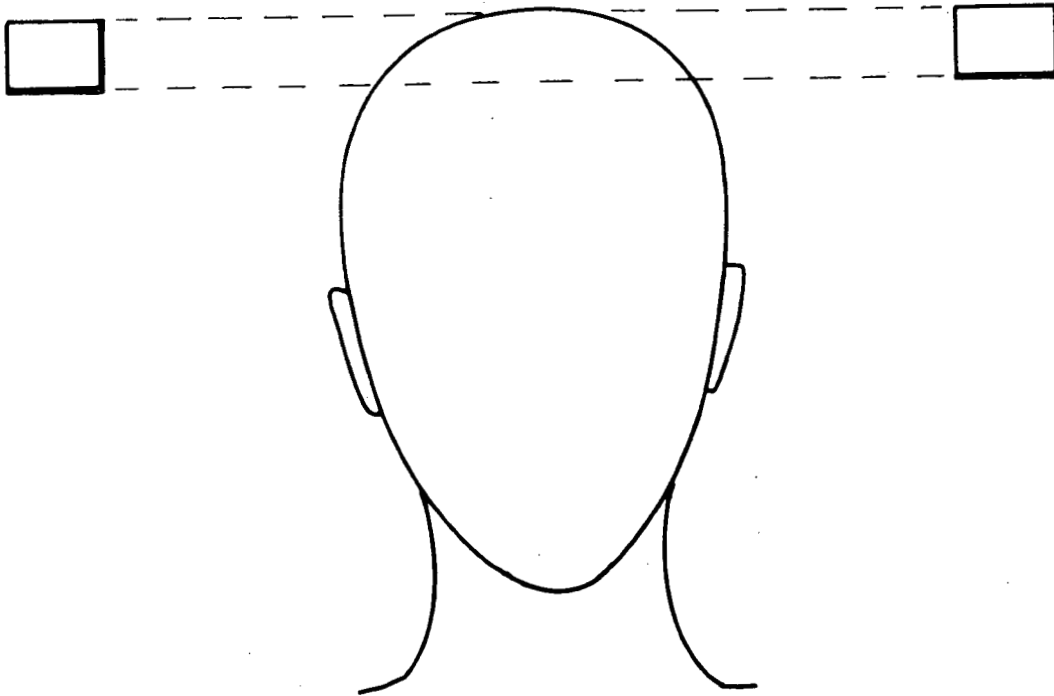


FIG. 1

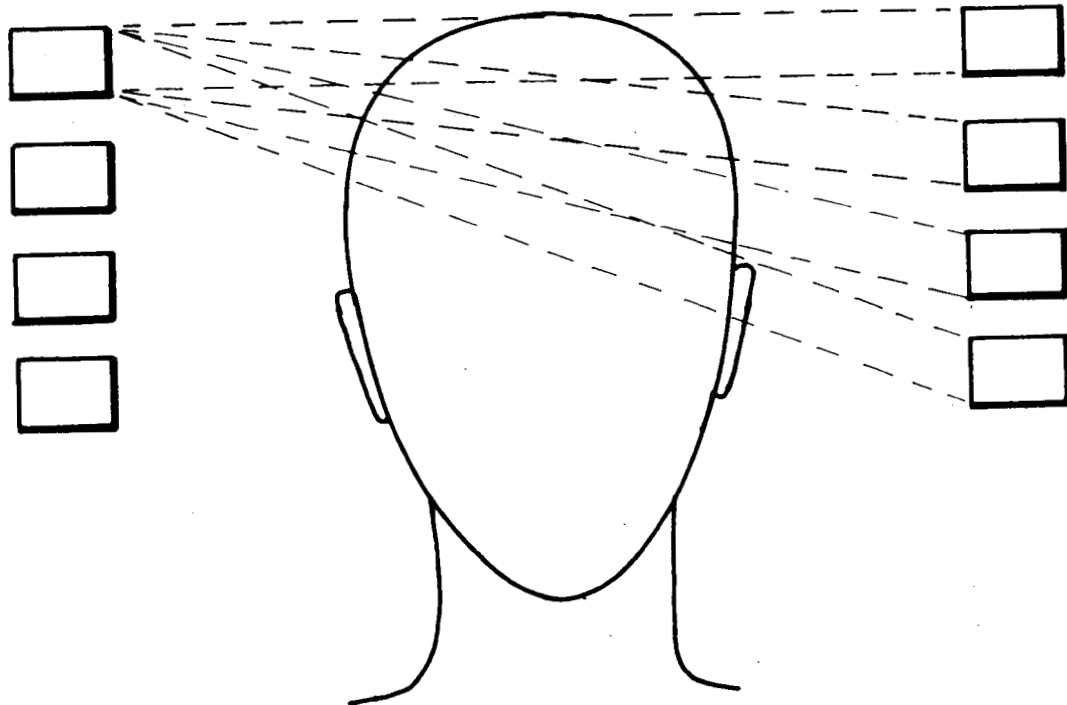


FIG. 2

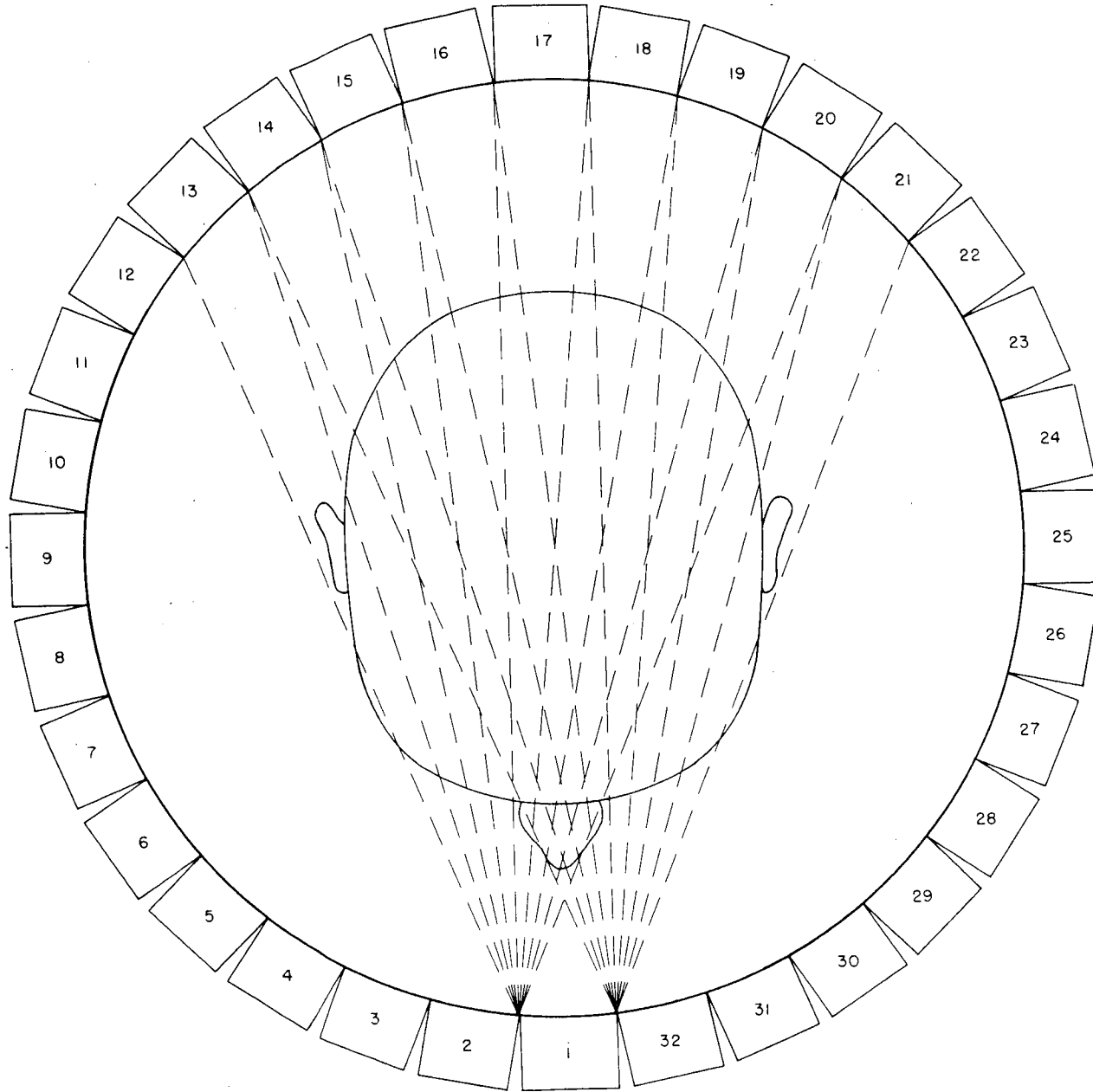


Fig 3

BNL Ne9. No. 3-371-62

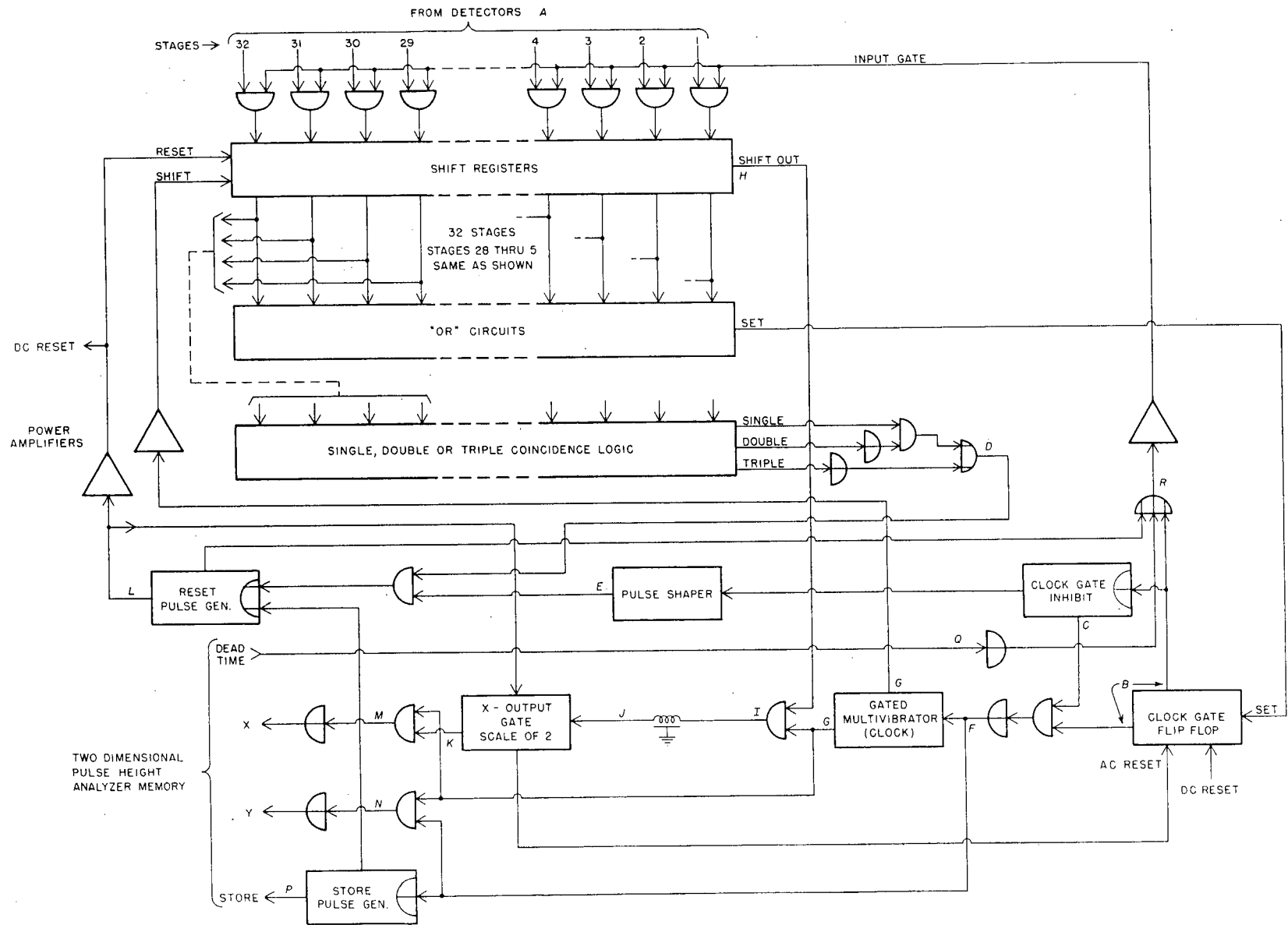


Fig 4

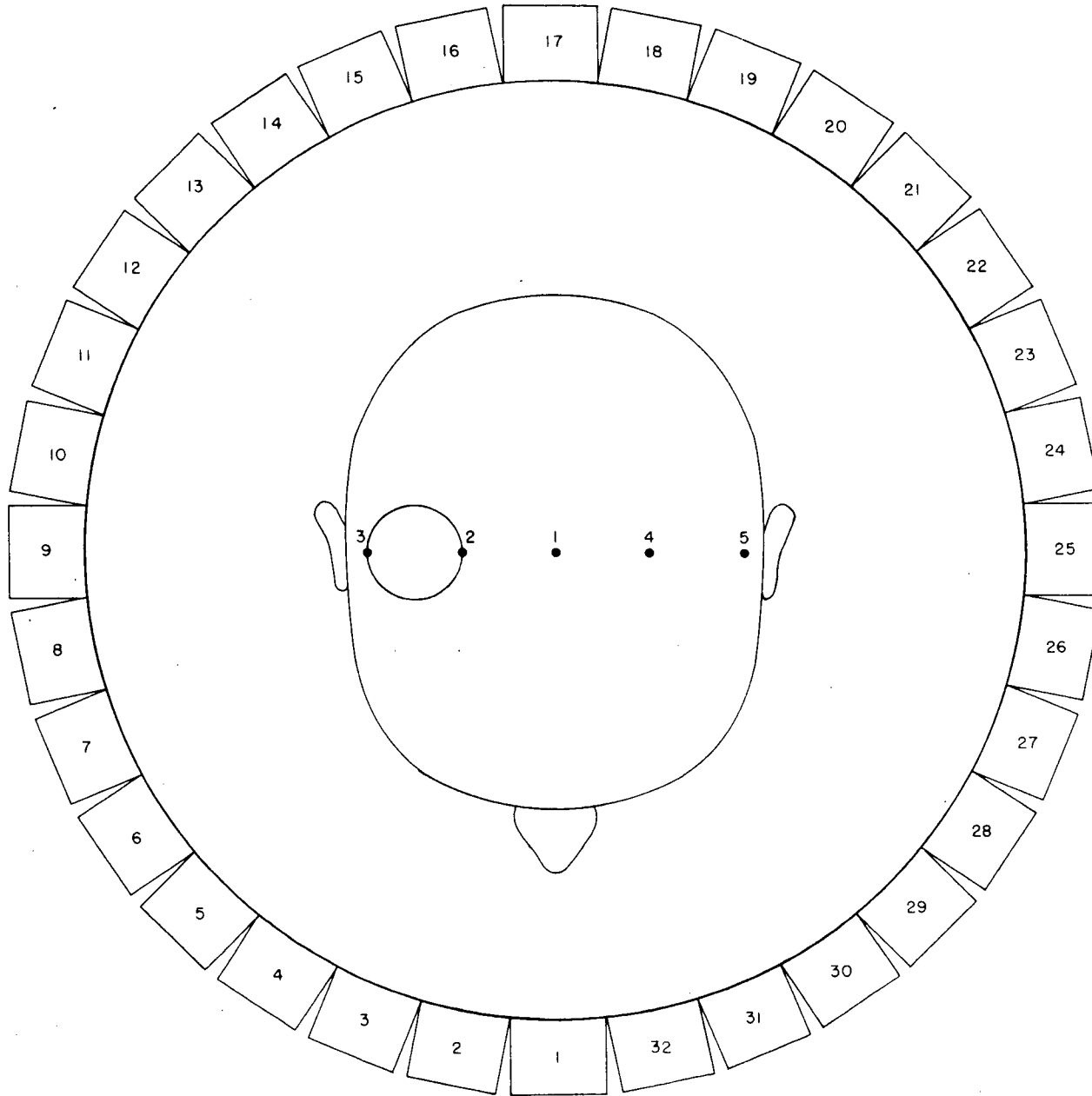


Fig 5  
BNC Neg. No. 9-370-62

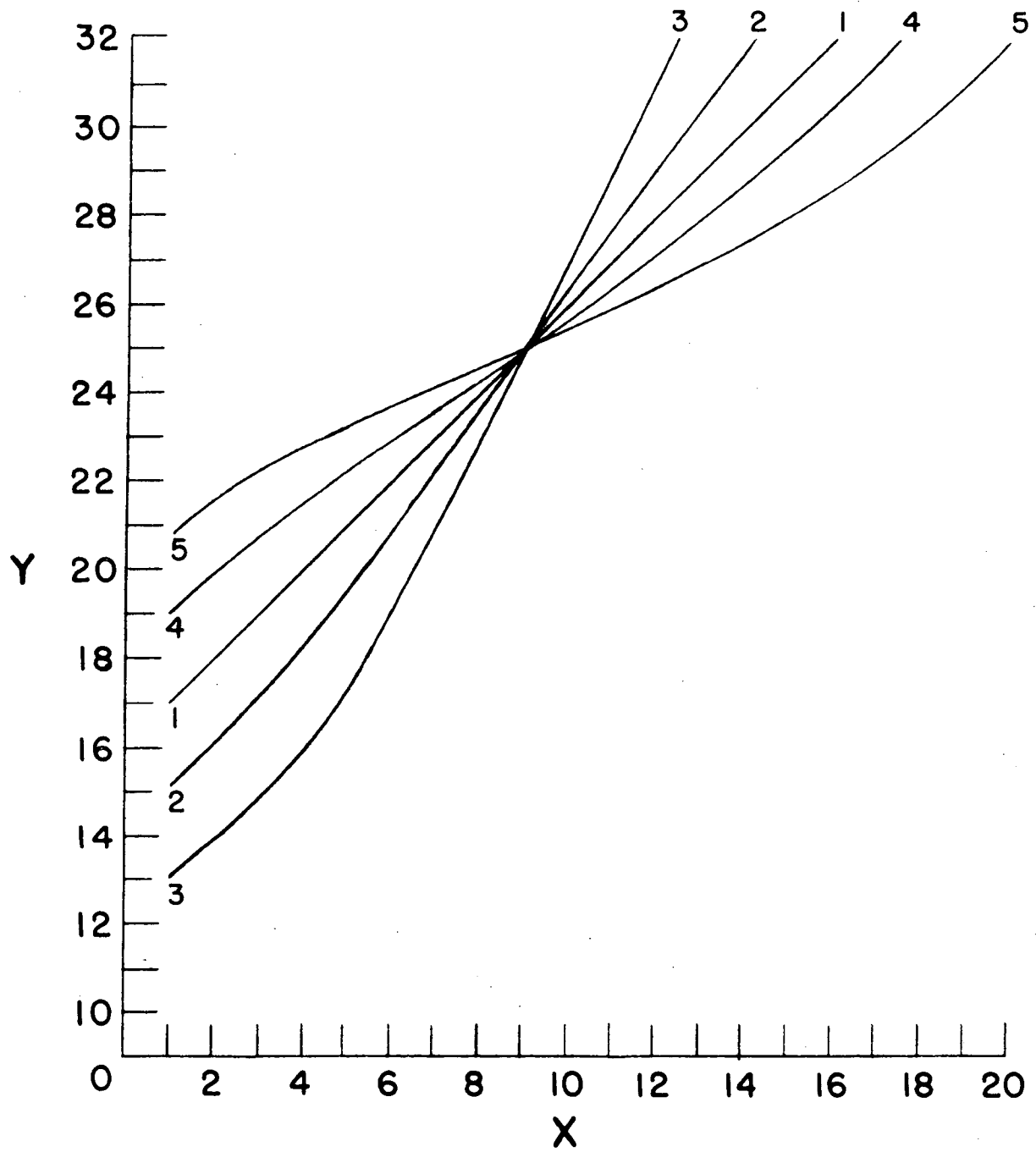


Fig 6  
BNV Neg. No. 3-374-62

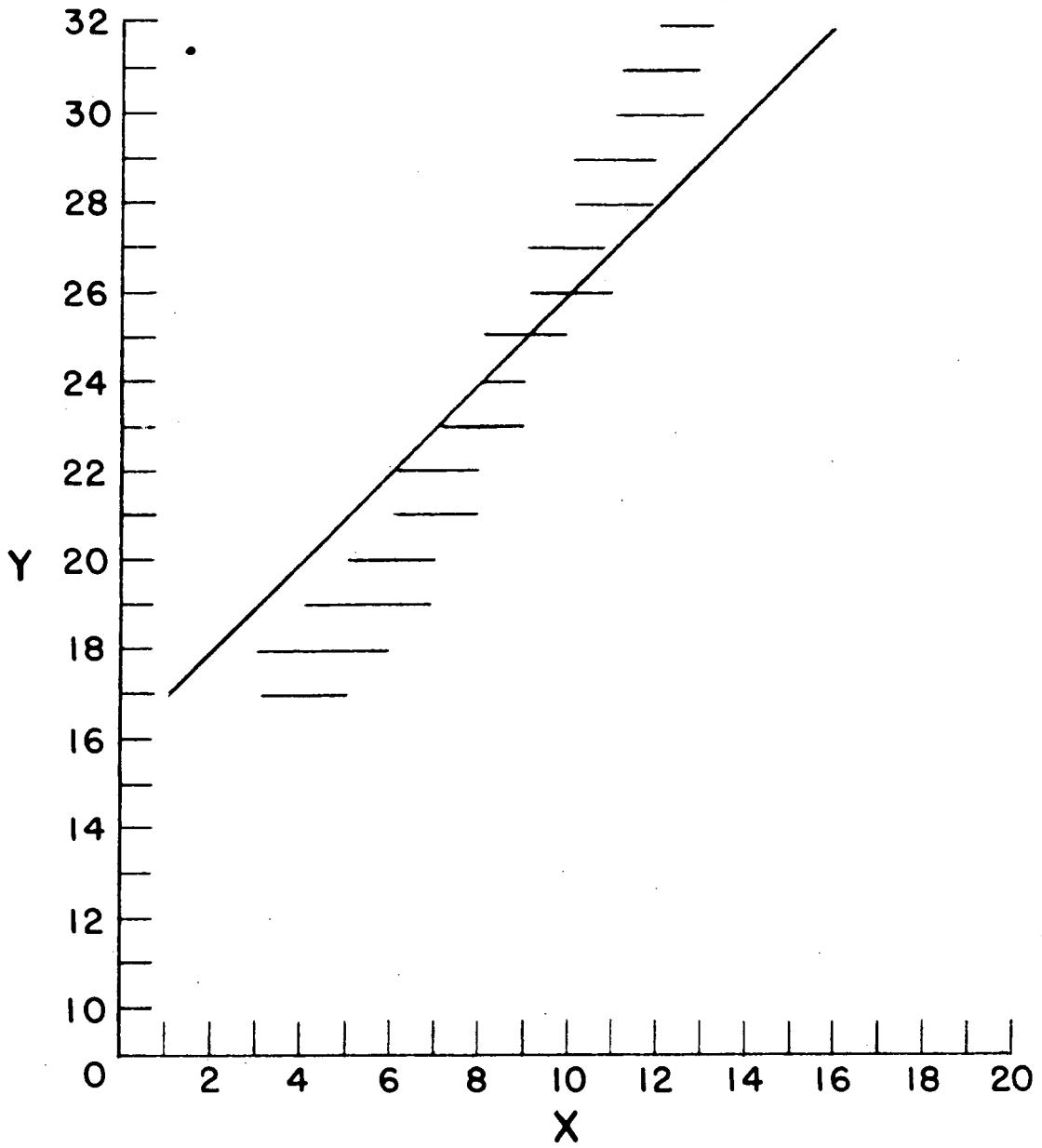


Fig 7  
BNL Neg. No. 3-37A-62

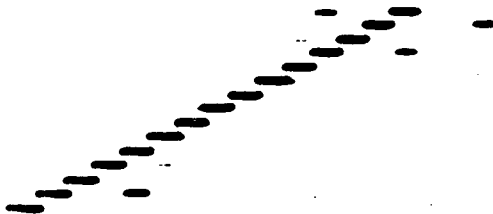
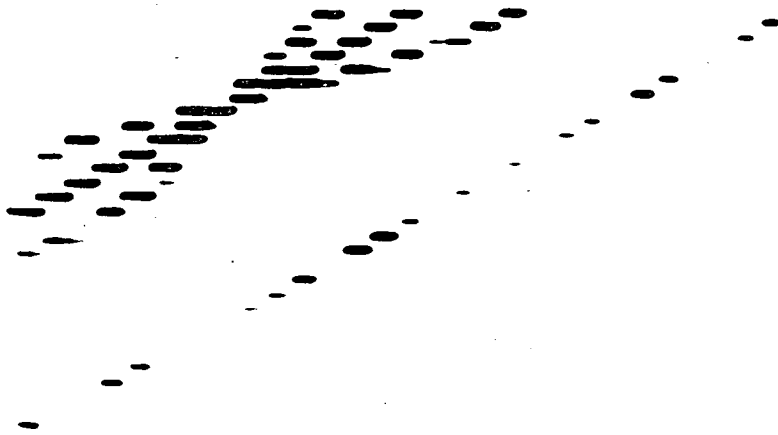
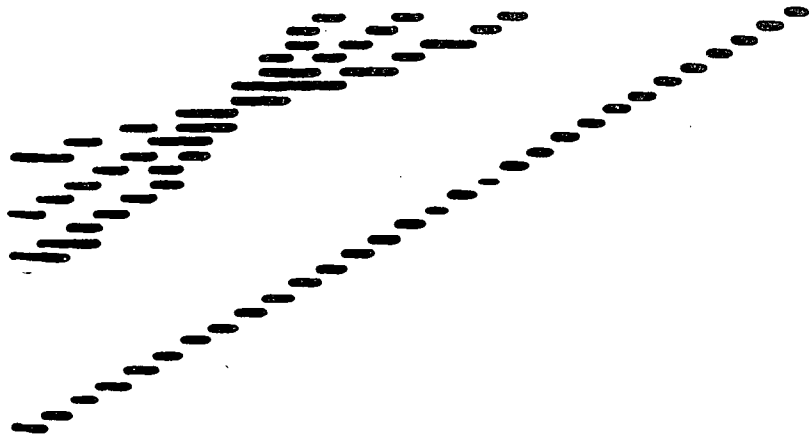


Fig 8a

Bill Neg. No 3-657-62.

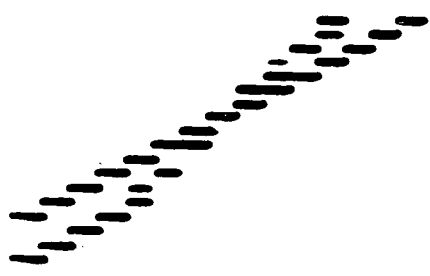
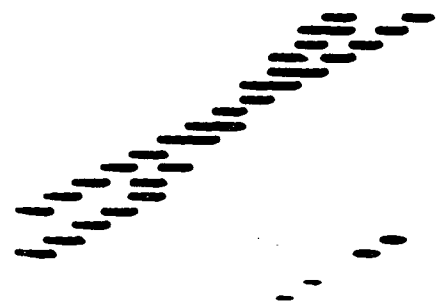
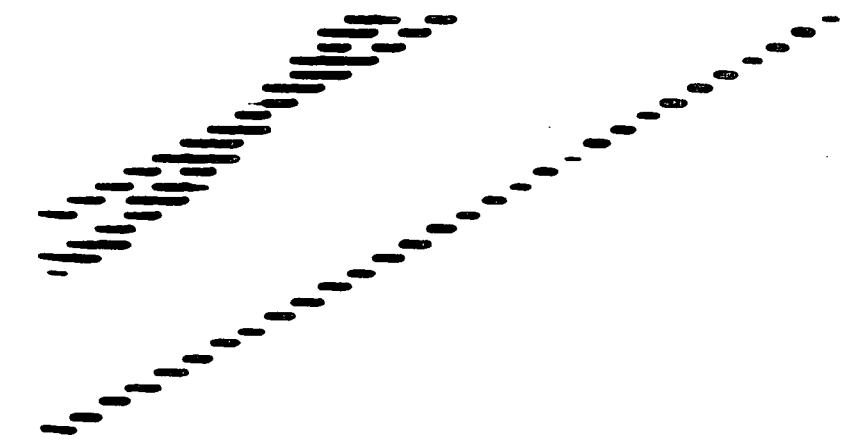


Fig 8b

BNC Neg. No. 3-658-62



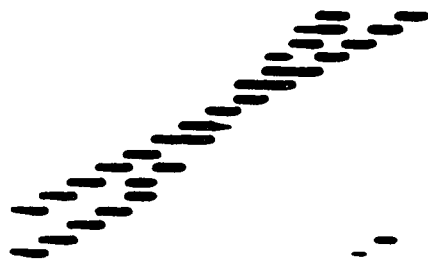
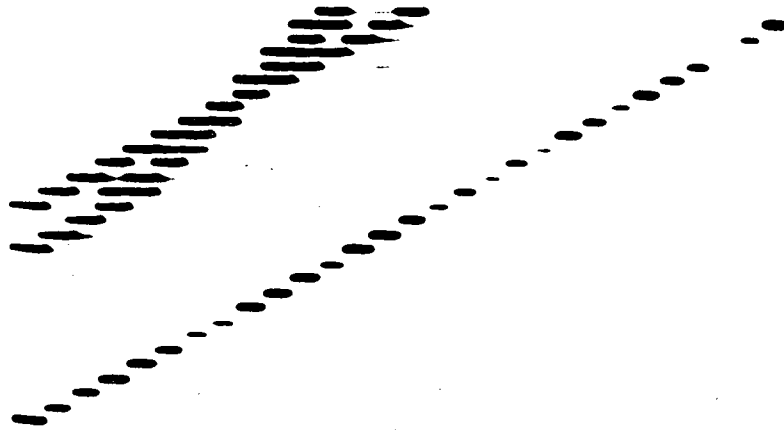


Fig 8 C  
Roll No. 211111



Fig 8 d  
RMI Neg. No. 3-650-62.

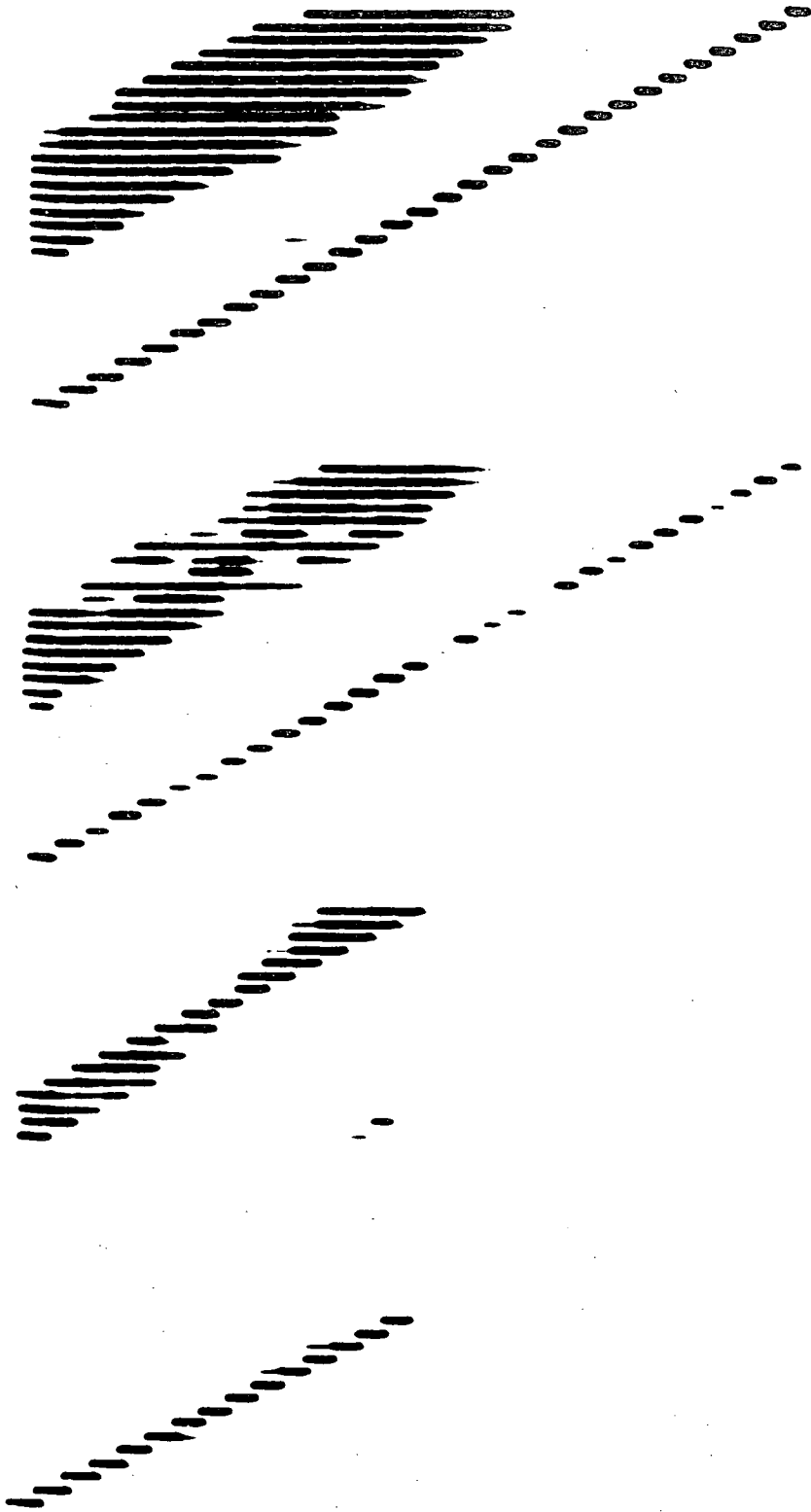


Fig 8 e  
BNI 1149.12 3-656-62.